

VLBI OBSERVATIONS OF GAMMA-RAY-QUIET AGN: COMPARING RADIO CORE BRIGHTNESS TEMPERATURES

S.J. Tingay and D.W. Murphy

Jet Propulsion Laboratory, California Institute of Technology

MS238-332, 4800 Oak Grove Dr., Pasadena CA, 91109-8099;

tingay@hyaa.jpl.nasa.gov, dwm@casa.jpl.nasa.gov

J.E.J. Lovell¹, M.E. Costa, and P. McCulloch

University of Tasmania, Hobart, 7001, Australia;

jlovell@vsop.isas.ac.jp, mcosta@kerr.phys.utas.edu, pmcc@physvax.phys.utas.edu

P.G. Edwards

Institute of Space and Astronautical Science, Sagamihara, Kanagawa 229, Japan;

pge@vsop.isas.ac.jp

D.L. Jauncey, J.E. Reynolds, A.K. Tzioumis, and E.A. King

CSIRO, Australia Telescope National Facility, Epping, 2121, Australia;

(djauncey, jreynold, atzioumi, eking)@atnf.csiro.au

D.L. Jones, R.A. Preston, D.L. Meier, and T.D. van Ommen

Jet Propulsion Laboratory, California Institute of Technology

MS238-332, 4800 Oak Grove Dr., Pasadena CA, 91109-8099;

dj@bllac.jpl.nasa.gov, rap@sgra.jpl.nasa.gov, dlm@cena.jpl.nasa.gov

G.D. Nicolson and J.F.H. Quick

¹Current address: Institute of Space and Astronautical Science, Sagamihara, Kanagawa 229, Japan

Hartebeesthoek Radio Astronomy Observatory, Krugersdorp, 1740, South Africa;

(george, jon)@bootes.hartrao.ac.za

Received _____; accepted _____

ABSTRACT

We present VLBI and Australia Telescope Compact Array images, and derive source frame radio-core brightness temperatures for three prominent, flat-spectrum extragalactic radio sources, notable because they have not been detected as gamma-ray sources with the EGRET instrument. Radio core brightness temperatures are discussed as an indicator of relativistic beaming.

A comparison of source frame radio-core brightness temperatures for EGRET-identified and gamma-ray-quiet, radio-loud AGN show that a wide range in beaming properties is likely to exist, independent of the level of gamma-ray emission. This comparison suggests that, although there is a strong relationship between radio emission and gamma-ray emission in EGRET-identified AGN, and that many EGRET-identified AGN show evidence for relativistic beaming, there is little evidence for a one-to-one correspondence between the strength of gamma-ray emission and the degree of beaming of the radio emission.

Subject headings: Radio continuum: galaxies – galaxies: active – galaxies: jets – galaxies: individual (PKS 0438–436, PKS 0637–752, PKS 1921–293) – Gamma-rays: observations – techniques: interferometric

1. INTRODUCTION

The study of gamma-ray emission from active galactic nuclei (AGN) has blossomed in recent years with the operation of the Energetic Gamma-Ray Experiment Telescope (EGRET), aboard the *Compton Gamma-Ray Observatory* (CGRO). EGRET has discovered greater than 100 MeV emission from over 120 discrete sources, identifying, with high confidence, 40 of those sources as strong, flat-spectrum extragalactic radio sources (Thompson et al. 1995; Thompson et al. 1996). Mattox et al. (1997) have carefully examined the claimed identifications and provide a list of 42 ‘robust’ EGRET detections which have either identifications with highly significant probabilities of being correct and/or corroborative evidence from other wavelengths to support the identification with the EGRET source.

The association between gamma-ray and radio emission in AGN has prompted much observational study of the properties of the EGRET-identified radio sources, and theoretical investigation into possible mechanisms for the production of gamma-rays in AGN. One of the areas of consideration in these investigations has been the search for differences between the EGRET-identified AGN and AGN which possess similar radio wavelength properties but have not been detected by EGRET. What makes a radio loud AGN gamma-ray bright?

Relativistic beaming has been suggested as a key feature in models for AGN gamma-ray emission and as a possible reason why some radio loud AGN are gamma-ray loud and others are not (e.g. Salamon & Stecker 1994; Fichtel et al. 1994 and references therein). If the gamma-ray emission originates deep within AGN jets and is relativistically beamed, as the observed short time-scale variability and extreme gamma-ray luminosities would suggest, then the apparent strength of gamma-ray emission from an AGN may be strongly orientation dependent; the strongest gamma-ray sources would be more aligned with our line of sight in this picture. It would seem reasonable, therefore, to search for differences

between the gamma-ray loud and gamma-ray-quiet, radio-loud AGN in terms of relativistic beaming indicators estimated from radio wavelength properties such as apparent jet speed, core brightness, and core brightness temperature etc, utilising VLBI techniques which can directly image the smallest linear scales in AGN, as close as is possible to the gamma-ray emission region (Moellenbrock et al. 1996; Tingay et al. 1996; Impey 1996; Mattox et al. 1997).

The results presented in this paper follow from our previous work (Tingay et al. 1996, hereafter T96) in which we compared the apparent jet speeds of gamma-ray quiet and gamma-ray loud radio AGN and found no significant difference. Here we extend our comparison of relativistic beaming indicators to include radio-core brightness temperatures (§2) since this line of investigation appears to be a promising one (Moellenbrock et al. 1996; Shen et al. 1997). To this end we present new VLBI data for three sources, of interest as prominent flat-spectrum radio sources which have not been detected as gamma-ray sources by EGRET (§3 & §4). Two of these sources were noted by von Montigny et al. (1995) in their comparison of gamma-ray loud and quiet radio sources, PKS 0438–436 and PKS 0637–752, respectively. We add a third source, PKS 1921–293, which is an extreme blazar. In order to discuss brightness temperatures in relation to the EGRET-identified radio sources we also review results from the literature (§5), in particular results from the first space VLBI observations (Linfield et al. 1989; Linfield et al. 1990).

Throughout this paper spectral index is defined as $S_\nu \propto \nu^\alpha$.

2. RADIO CORE BRIGHTNESS TEMPERATURES

Relativistic beaming can be measured in terms of the Doppler factor, δ , which relates the intensity in the observer’s frame to the intensity in the rest frame, of radiation

originating from material traveling at a significant fraction of the speed of light, such as the radio emission from a relativistic jet,

$$\frac{S_{c.f.}}{S_{jet}} = \delta_{jet}^{3-\alpha} = \frac{1}{\gamma^{3-\alpha}(1-\beta\cos\theta)^{3-\alpha}} \quad ; \quad \nu_{c.f.} = \delta_{jet}\nu_{jet} \quad ,$$

for a spherical component, where $S_{c.f.}$ is the intensity in the co-moving frame of the source; S_{jet} is the intensity in the rest frame of the jet; γ and β have their usual definitions in relativity and refer to the motion of the radiating material (e.g. Blandford & Konigl 1979); θ is the angle the material motion makes to the line of sight; α is the spectral index of the emission; and ν is the frequency of radio emission. The degree of beaming or amplification of the intrinsic intensity increases as $\beta \rightarrow 1$ and $\theta \rightarrow 0$.

The measurement of radio-core brightness temperatures with high-resolution VLBI observations may provide a lower limit estimate of the Doppler factor, δ_{jet} , under the usual assumption that the core is the region of the jet where radio emission is first produced. The observed radio-core brightness temperature can be written as (Murphy 1993)

$$T_{12,o.f.} = \frac{1.22S_{o.f.}}{ab\nu_{o.f.}^2} \quad ,$$

where $S_{o.f.}$ is the flux density (in Jy) from a radio-core at the frequency $\nu_{o.f.}$ (in GHz) in the observers frame; a and b are the semi-major and semi-minor axes of the core component (in mas); and $T_{12,o.f.}$ is the brightness temperature in the observer's frame, in units of 10^{12} K. If the radio-core appears bright as a result of beamed emission then, using the above equations,

$$T_{12,o.f.} = \frac{1.22S_{jet}}{(1+z)^{1-\alpha}ab\nu_{jet}^2}\delta_{jet}^{1-\alpha} \quad .$$

where $1/(1+z)$ is the cosmological Doppler factor which has to be taken into account for high redshift sources, making the overall Doppler factor $\delta_{jet}/(1+z)$. If the

rest-frame brightness temperature is limited by inverse-Compton scattering losses to approximately 10^{12} K, as argued by Kellermann & Pauliny-Toth (1969), it follows that if $T_{12,o.f.}(1+z)^{1-\alpha} > 1$ then $\delta_{jet}^{1-\alpha} > T_{12,o.f.}(1+z)^{1-\alpha}$. In this case, a lower limit for the Doppler factor can be estimated from the three quantities $T_{12,o.f.}$, z , and α .

It should be noted that alternatives to the above scheme have been suggested. For example, Slysh (1992) proposes that non-stationary conditions in radio-loud AGN may produce extremely high radio-core brightness temperatures, orders of magnitudes greater than the nominal inverse Compton limit for short periods of time. Coherent stimulated emission processes have also been proposed as a alternative to incoherent synchrotron emission (e.g. Baker et al. 1988).

3. OBSERVATIONS AND ANALYSIS

A log of our VLBI observations appears in Table 1 with a list of the radio telescopes used from the Southern Hemisphere VLBI Network array (Preston et al. 1989; Jauncey et al. 1994). The resulting data were obtained and reduced to images and radio-core brightness temperatures as described in T96. The typical error on the formal Gaussian fits to the radio-core major and minor axes was between 0.01 and 0.05 mas for each of the sources described here, resulting in an error in the derived observed brightness temperature of between 10% and 20%.

We also obtained Australia Telescope Compact Array (ATCA) imaging observations at 4.80 and 8.64 GHz for two of the sources, PKS 0438–436 (1993 March 1) and PKS 0637–752 (1993 July 13). The observations were made with a 6 km array, a 128 MHz bandwidth, and recording XX, YY, XY, and YX linear polarization products. The primary calibrator for the ATCA, PKS 1934–638, was used to calibrate the amplitude scale for the

observations. The data were reduced in AIPS and images were subsequently made using the DIFMAP software (Shepherd, Pearson & Taylor 1994).

Additional ATCA observations, also with a 6 km configuration, were made at 1.43, 2.32, 4.85, and 8.69 GHz on 1996 October 12 for the three sources described here plus the sources described in T96, to determine the radio-core spectral indices. These data were reduced in the MIRIAD package (Sault & Killeen 1996). The observations consisted of one 2 min observation per source, thus image formation was not possible.

4. THE INDIVIDUAL SOURCES

4.1. PKS 0438–436

PKS 0438–436 is one of the bright, flat-spectrum radio sources considered by von Montigny et al. (1995) to be of interest as a blazar not detected by EGRET; Fichtel et al. (1994) place a 2σ upper limit of $0.7 \times 10^{-7} \text{ cm}^{-2}\text{s}^{-1}$ for > 100 MeV emission from combined Phase 1 EGRET observations. PKS 0438–436 is a high redshift, and consequently high luminosity, radio-loud quasar at $z=2.852$ (Morton, Savage, & Bolton 1978). It exhibits the typical blazar characteristic of high and variable optical polarization (Impey & Tapia 1988). PKS 0438–436 remains bright at a wavelength of 3 mm, with a flux density of 1.49 Jy (Beasley et al. 1997).

The 1982 multi-baseline VLBI observations at 2.3 GHz by Preston et al. (1989) with the SHEVE array were used to produce both a model and an image of PKS 0438–436. Preston et al. found that the compact source consisted of two 1.9 Jy components separated by 35 mas at a position angle of -43° , with the south-east component slightly more extended than the north-west component. They also found a large position angle difference between the VLBI structure and a $2''$ extension at a position angle of approximately 10°

observed with the VLA (Perley 1985). The angular length and position angle of this arcsecond extension has been confirmed with our 8.4 GHz observations at the ATCA (Figure 1).

VLBI images obtained in 1989, again at 2.3 GHz, showed no significant change in the structure of the radio source, although both components remained essentially unresolved at this resolution (Murphy et al. 1993).

The 4.8 GHz VLBI data from 1992 November presented here (Figure 2) show the two components seen previously at lower frequency by Preston et al. (1989) and Murphy et al. (1993). The south-east component is less compact than the flat-spectrum north-west component, which we identify as the core of the radio source. The two components are both elongated, but not along the same position angle. The north-west component has a position angle of approximately 124° whereas the south-east component has a position angle of approximately 35° . The position angle connecting the centroids of the two components is approximately 136° , agreeing well with the results of Preston et al. (1989) and Murphy et al. (1993) (Preston et al. and Murphy et al. could not distinguish the core and therefore list -43° as the position angle). The distance between the centroids of the two components in Figure 2 is 36.2 mas, only 1.2 mas greater than in 1982. The mismatch in frequency and resolution between these observations does not allow any meaningful estimate of the apparent speed of separation between these components.

From Figure 2, the core FWHM and integrated flux density have been estimated to be 0.6×0.2 mas and 1.6 Jy, respectively. The observed radio-core brightness temperature is therefore approximately 7.0×10^{11} K at 4.8 GHz. The core spectral index between 4.8 and 8.6 GHz on 1996 October 12 was 0.3.

The misalignment between the VLBI and VLA radio structures noted by Preston et al. (1989) is continued on the mas-scale between the two compact components. The

misalignment between the mas-scale and arcsecond-scale structures is approximately 126° . The misalignment on the mas scale, between the two components, is approximately 89° .

4.2. PKS 0637–752

PKS 0637–752 ($z=0.651$; Savage, Browne, & Bolton 1976) is another of the strong, flat-spectrum radio sources considered by von Montigny et al. (1995) in their investigation of radio sources not identified by EGRET. The 2σ upper limit for > 100 MeV emission from this source during EGRET Phase 1 observations is $0.4 \times 10^{-7} \text{ cm}^{-2}\text{s}^{-1}$ (Fichtel et al. 1994). The radio source remains bright at mm wavelengths with 1.76 Jy at 3 mm and 1.01 Jy at 2 mm (Beasley et al. 1997).

4.8 GHz imaging of the kpc-scale radio structure with the ATCA shows a strongly one-sided jet which lies at a position angle of approximately -86° (Figure 3).

The compact structure of the radio source was first revealed by Preston et al. (1989) with multi-baseline 2.3 GHz VLBI observations using the SHEVE array. They reported an essentially unresolved component with a 2.6 Jy core and a halo of emission greater than 20 mas in extent with a flux density of 1.5 Jy. Our 1993 May VLBI observations (Figure 4) at the higher frequency of 4.8 GHz show that the compact radio structure is dominated by a bright core and a jet lying at a position angle of approximately -90° . The mas-scale and arcsecond-scale radio structures are very well aligned, the difference in position angle being approximately 4° .

From Figure 4, the core FWHM and total flux density, de-convolved from the restoring beam, have been estimated at 0.4×0.4 mas and 4.3 Jy, respectively, leading to a value for the observed radio-core brightness temperature of approximately 1.5×10^{12} K at the frequency of 4.8 GHz. The core spectral index between 4.8 and 8.6 GHz on 1996 October

12 was 0.2.

Again the mismatch in resolution and data quality between these images and the model of Preston et al. (1989) does not allow a useful estimate of apparent motion to be made for this source.

4.3. PKS 1921–293

PKS 1921–293 (OV-236) is one of the strongest (up to ~ 25 Jy at cm wavelengths), flat-spectrum radio sources in the sky, but was not detected by EGRET in greater than 100 MeV gamma-rays. It is a highly polarized and, optically, violently variable quasar at a redshift of $z=0.352$ (Wills & Wills 1981). Fichtel et al. (1994) place an upper limit to greater than 100 MeV emission from PKS 1921–293 of $0.6 \times 10^{-7} \text{ cm}^{-2}\text{s}^{-1}$, from Phase I EGRET observations. It was not considered by von Montigny et al. (1995) in their investigation of radio sources not identified by EGRET, since PKS 1921–293 does not appear in their 1 Jy compendium (it lies at a galactic latitude of just under 10°), whereas they did consider the similar sources PKS 0438–436 and PKS 0637–752.

PKS 1921–293 was observed by Preston et al. (1989) with the first multi-baseline VLBI observations at a frequency of 2.3 GHz. They found the radio source to consist of a 5 mas elongated component at a position angle of approximately 25° and with a flux density of 6.6 Jy. Our 1993 February VLBI observations at 4.8 GHz are shown in Figure 5. The image shows that the compact radio source is dominated by an unresolved core component and a jet-like structure at a position angle of approximately 25° , agreeing with the results of Preston et al. (1989). PKS 1921–293 was completely unresolved at the VLA at 1.4 and 5 GHz as observed by de de Pater, Schloerb & Johnston (1985) and Perley (1982), and so no comparison can be made between the mas-scale and arcsecond-scale structure position

angles.

From Figure 5, the core dimensions and flux density, de-convolved from the restoring beam, are $< 0.5 \times < 0.5$ mas and 9.4 Jy. These values give an observed radio-core brightness temperature of $> 1.9 \times 10^{12}$ K at the frequency of 4.8 GHz. The core spectral index between 4.8 and 8.6 GHz on 1996 October 12 was 0.0.

PKS 1921–293 has the highest lower limit on observed brightness temperature of the three radio sources considered here. Previously Moellenbrock et al. (1996) found that PKS 1921–293 had the highest 22 GHz correlated flux density and observed brightness temperature in their sample of 140 sources, 12.6 ± 1.6 Jy and $> 7 \pm 2^4 \times 10^{12}$ K, respectively.

The high brightness temperature inferred from ground-based VLBI observations is confirmed from VLBI observations with greater than Earth diameter baselines. From the TDRSS space VLBI experiments, Linfield et al. (1989) found that PKS 1921–293 had a source frame brightness temperature of approximately 3.8×10^{12} K at a frequency of 2.3 GHz, the highest observed in this experiment for the sources with measured redshifts.

5. DISCUSSION AND CONCLUSIONS

Table 2 contains the estimates of observed radio-core brightness temperature in units of 10^{12} K, $T_{12,o.f.}$, for the gamma-ray-quiet radio sources described in §4, as well as those EGRET-identified radio sources described in T96. Included in Table 2 are the corresponding co-moving frame brightness temperatures, $T_{12,c.f.}$, and lower limits for the jet Doppler factor, δ_{jet} . From these data there is no indication that the degree of radio emission beaming in the EGRET-identified radio sources is higher than for the gamma-ray-quiet, radio-loud sources.

On the other hand, Moellenbrock et al. (1996) list the *observed* brightness temperatures, or lower limits, for 140 compact radio sources derived from 22 GHz intercontinental VLBI

observations and plot their distribution. The 21 EGRET-identified radio sources in their sample tend towards the high-brightness-temperature end of this distribution, although many of the bright and high-brightness-temperature sources in their sample are gamma-ray-quiet, including PKS 1921–293.

To put these two results into context it should be noted that there are well-known limitations associated with estimating high brightness temperatures with ground-based interferometers (Linfield et al. 1989). To accurately measure brightness temperatures, higher than 10^{12} K, the need arises for VLBI baseline lengths which can be achieved only by using radio telescopes in Earth orbit. Limited space VLBI observations have been undertaken previously, in an experiment using the TDRSS satellite in conjunction with ground-based telescopes (Levy et al. 1986). Linfield et al. (1989; 1990) report on the measurement of *co-moving frame* radio-core brightness temperatures from these observations.

At 2.3 GHz, Linfield et al. (1989) detected 23 out of 24 sources observed and could derive Gaussian models and therefore brightness temperatures for 14. Three of these sources have been identified as gamma-ray sources. The brightness temperatures of the three gamma-ray sources, 0336–019, 0420–014 and 3C 279, are midrange in the sample, 2.03×10^{12} K, 3.14×10^{12} K and 1.59×10^{12} K, respectively. The brightness temperatures for the remaining 12 sources ranged between 2.5×10^{11} K (0723–008) and 3.80×10^{12} K (PKS 1921–293), for those sources with measured redshifts. 0336–019, 0420–014 and 3C 279 were the fifth, third, and seventh highest brightness temperature objects, respectively, of the sources with measured redshifts.

At 15 GHz, Linfield et al. (1990) were able to derive Gaussian models and brightness temperatures for nine sources from the TDRSS data. Four of the nine are identified gamma-ray sources. Again, the brightness temperatures for these sources, 3C 273, 3C 279,

1510–089, and 1730–130 are midrange for the sample, 1.14×10^{12} K, 1.98×10^{12} K, 1.55×10^{12} K, and 8.7×10^{11} K, respectively. The remaining five sources are gamma-ray-quiet and have 15 GHz brightness temperatures ranging between 7.5×10^{11} K (0823+033; a redshift of 0.506 has been found since Linfield et al reported their results) and 2.40×10^{12} K (3C 446). The ranking of the gamma-ray sources in brightness temperature was sixth, fourth, fifth, and seventh, respectively, of the sources with measured redshifts.

The conclusion we draw from the results of Linfield et al. (1989, 1990), Moellenbrock et al. (1996), and the current study, is that, although there appears to exist a trend relationship between relativistically beamed radio emission and gamma-ray emission in AGN, there is no one-to-one correspondence. This point can be illustrated by two sources: PKS 1921–293 is consistently found to be one of the most highly beamed radio sources from VLBI measurements of brightness temperature (Table 2; Moellenbrock et al. 1996; Linfield et al. 1989) but has not been detected with the EGRET instrument. On the other hand PKS 0521–365, which has been identified by EGRET does not require relativistic beaming to explain its radio-core brightness temperature.

A wide range in brightness temperature exists, independent of the strength of gamma-ray emission, at least in AGN which are among the most prominent at radio wavelengths. Thus, relativistic beaming is not the only factor which affects the presence, absence or apparent strength of gamma-ray emission in AGN. A paradigm in which all radio-loud AGN produce gamma-rays, and their detectability caused only by the degree of relativistic beaming, is not tenable. Other, perhaps intrinsic, processes must also play a role. For instance, AGN may only produce gamma-rays during high-output states, which could explain, equally well as relativistic beaming, the significant difference in observed radio flux density between the EGRET-identified and gamma-ray-quiet radio sources (Impey 1996; Mattox et al. 1997). In this picture, every flat-spectrum radio source will at

some stage become a gamma-ray source and those sources which are currently very bright at radio wavelengths but gamma-ray-quiet, like PKS 0436–438, 0637–752, and 1921–293 were, possibly, gamma-ray bright in the recent past.

Long-term multiwavelength variability studies, as well as space VLBI observations of complete samples, should be used to test this idea. Those sources which are currently gamma-ray bright may have had lower radio flux densities than in the past, which they may return to after weakening in gamma-rays.

6. SUMMARY

We have presented VLBI images for three prominent, flat-spectrum, radio-loud AGN which have not been detected above 100 MeV by EGRET, and compared their source frame brightness temperatures with three radio-loud AGN positively identified by EGRET, and observed by us previously. The radio-core brightness temperatures are an indicator of relativistic beaming and show that the most highly beamed radio sources are not necessarily gamma-ray sources. This result is strengthened by the existing VLBI data on Earth-space baselines, which are more reliable than ground-based measurements. Mechanisms intrinsic to the source, in addition to relativistic beaming, must be held accountable for the gamma-ray properties of AGN.

7. ACKNOWLEDGMENTS

We express our gratitude to the time-assignment committees of the participating observatories, the management of the Deep Space Network, and Telstra (Australia). We also thank the staff of the Caltech/JPL correlator. We would like to thank L. Kedziora-Chudczer and D. Goddard for careful proofreadings and helpful comments.

S.J.T. and J.E.J.L. acknowledge support via Australian Postgraduate Awards and the Australia Telescope National Facility student program. Part of this work was undertaken while S.J.T. held a National Research Council – JPL/NASA Research Associateship. P.G.E. acknowledges receipt of a Monbusho Fellowship. We also acknowledge support from the Perth Astronomy Research Group and the Australian Research Council. The Australia Telescope is operated as a national facility by CSIRO. Part of this research was carried out at the Jet Propulsion Laboratory, California Institute of Technology, under contract with the National Aeronautics and Space Administration. This research has made use of the NASA/IPAC Extragalactic Database (NED) which is operated by the Jet Propulsion Laboratory, California Institute of Technology, under contract with the National Aeronautics and Space Administration.

REFERENCES

- Baker, D.N., Borovsky, J.E., Benford, G., & Eilek, J.A. 1988, ApJ, 326, 110
- Beasley, A.J., Conway, J.E., Booth, R.S., & Nyman, L-Å 1997. A&A, in press
- Blandford, R.D. & Konigl, A. 1979, ApJ, 232, 34
- de Pater, I., Schloerb, F.P., & Johnston, A.H. 1985, AJ, 90, 846
- Fichtel, C.E. et al. 1994, ApJS, 94, 551
- Impey, C.D. 1996, AJ, 112, 2667
- Impey, C.D. & Tapia, S. 1988, ApJ, 333, 666
- Jauncey, D.L. et al. 1994, in IAU Symp. 158, Very High Angular Resolution Imaging, eds
J.G. Robertson & W.J. Tango (Dordrecht: Kluwer), 131
- Kellermann, K.I. & Pauliny-Toth, I.I.K. 1969, ApJ, 155, L71
- Levy, G.S. et al. 1986, Science, 234, 117
- Linfield, R.P. et al. 1989, ApJ, 336, 1105
- Linfield, R.P. et al. 1990, ApJ, 358, 350
- Mattox, J.R., Schachter, J., Molnar, L., Hartman, R.C., & Patnaik, A.R. 1997, ApJ, 481,
95
- Mollenbrock, G.A. et al. 1996, AJ, 111, 2174
- Morton, D.C., Savage, A. & Bolton, J.G. 1978, MNRAS, 185, 735
- Murphy, D.W. 1993, JPL interoffice memorandum, 'Model-fitting with RadioAstron',
http://sgra.jpl.nasa.gov/mosaic_v0.0/JPL_Project_dir/memo_ps.html

- Murphy, D.W. et al. 1993, in ‘Sub-arcsecond radio astronomy’, Eds.: R.J. Davis & R.S. Booth (Cambridge University Press), 243
- Perley, R.A. 1982, AJ, 87, 859
- Perley, R.A. 1985, private communication in Preston et al. (1989)
- Preston, R.A. et al. 1989, AJ, 98, 1
- Sault, R. & Killeen, N. 1996, MIRIAD users manual,
<http://www.atnf.csiro.au/Software/Analysis/miriad>
- Salamon, M. & Stecker, F.W. 1994, ApJ, 430, L21
- Savage, A., Browne, I.W.A., & Bolton, J.G. 1976, MNRAS, 177, 77p
- Shepherd, M.C., Pearson, T.J., & Taylor, G.B. 1994, BAAS, 26, 987
- Shen, Z.-Q. et al. 1997, AJ, in press
- Slysh, V.I. 1992, ApJ, 391, 453
- Thompson, D.J. et al. 1996, ApJS, 107, 227
- Thompson, D.J. et al. 1995, ApJS, 101, 259
- Tingay, S.J. et al. 1996, ApJ, 464, 170 (T96)
- von Montigny, C. et al. 1995, A&A, 299, 680
- Wills, D. & Wills, B.J. 1981, Nature, 289, 384

FIGURE CAPTIONS

Figure 1 ATCA image of PKS 0438–436 at 8.6 GHz from 1993 March 1. Contours -0.25, 0.25, 0.5, 1, 2, 4, 8, 16, 32, and 64% of peak, 3.6 Jy beam^{-1} . Beam, $2.''57 \times 0.''95$ at a position angle of 7.9° . The crosses are the positions of the clean components.

Figure 2 VLBI image of PKS 0438–436 at 4.8 GHz from 1992 Nov. 26. Contours -1, 1, 2, 4, 8, 16, 32, and 64% of peak, 1.6 Jy beam^{-1} . Beam, $3.2 \times 2.6 \text{ mas}$ at the position angle of -13.8°

Figure 3 ATCA image of PKS 0637–752 at 4.8 GHz from 1993 July 13. Contours 0.25, 0.5, 1, 2, 4, 8, 16, 32, and 64% of peak, 5.6 Jy beam^{-1} . Beam, $2.''25 \times 1.''98$ at the position angle of -22.7°

Figure 4 VLBI image of PKS 0637–752 at 4.8 GHz from 1993 May 15. Contours -1, 1, 2, 4, 8, 16, 32, and 64% of peak, 3.6 Jy beam^{-1} . Beam, $1.9 \times 0.6 \text{ mas}$ at the position angle of 7.3°

Figure 5 VLBI image of PKS 1921–293 at 4.8 GHz from 1993 Feb. 15. Contours 1, 2, 4, 8, 16, 32, and 64% of peak, 7.9 Jy beam^{-1} . Beam, $3.5 \times 0.7 \text{ mas}$ at the position angle of 4.2°

Source	Epoch	Frequency (GHz)	Participating Telescopes
PKS 0438–436	1992 Nov. 26	4.851	At,Mp,Pa,Ho,Pr27
PKS 0637–752	1993 May 15	4.851	At,Mp,Pa,Ho,Pr27,Hh
PKS 1921–293	1993 Feb. 15	4.851	At,Mp,Pa,Ho,Pr27,Hh

Table 1: Observation log for EGRET and non-EGRET sources: Pa = Parkes (64 m, ATNF), Ho = Hobart (26 m, Uni. Tas.), At = Narrabri (22 m, ATNF), Mp = Mopra (22 m, ATNF), Pr27 = Perth (27 m, ESA), Pr15 = Perth (15 m, Telstra), Hh = Hartebeesthoek (26 m, HRAO)

source	z	EGRET detection	$T_{12,o.f.}$	${}_{4.8}^{8.6}\alpha_{core}$	$T_{12,c.f.}$	δ_{jet}
PKS 0208–512	1.003	strong	>1.2	-0.1	>2.6	>2.4
PKS 0438–436	2.852	none	0.7	0.3	1.8	>2.3
PKS 0521–365	0.055	weak	0.1	0.0	0.1	N/A
PKS 0537–441	0.894	strong	0.7	0.2	1.2	>1.3
PKS 0637–752	0.651	none	1.5	0.2	2.2	>2.7
PKS 1921–293	0.352	none	>1.9	0.0	>2.6	>2.6

Table 2: VLBI and EGRET properties of the 6 sources, *Column 1* Source name, *Column 2* Source redshift, *Column 3* EGRET detection, *Column 4* Observed brightness temperature in units of 10^{12} K, *Column 5* Core spectral index between 4.8 and 8.6 GHz, *Column 6* Source frame brightness tempearure in units of 10^{12} K, *Column 7* Lower limit on jet Doppler factor

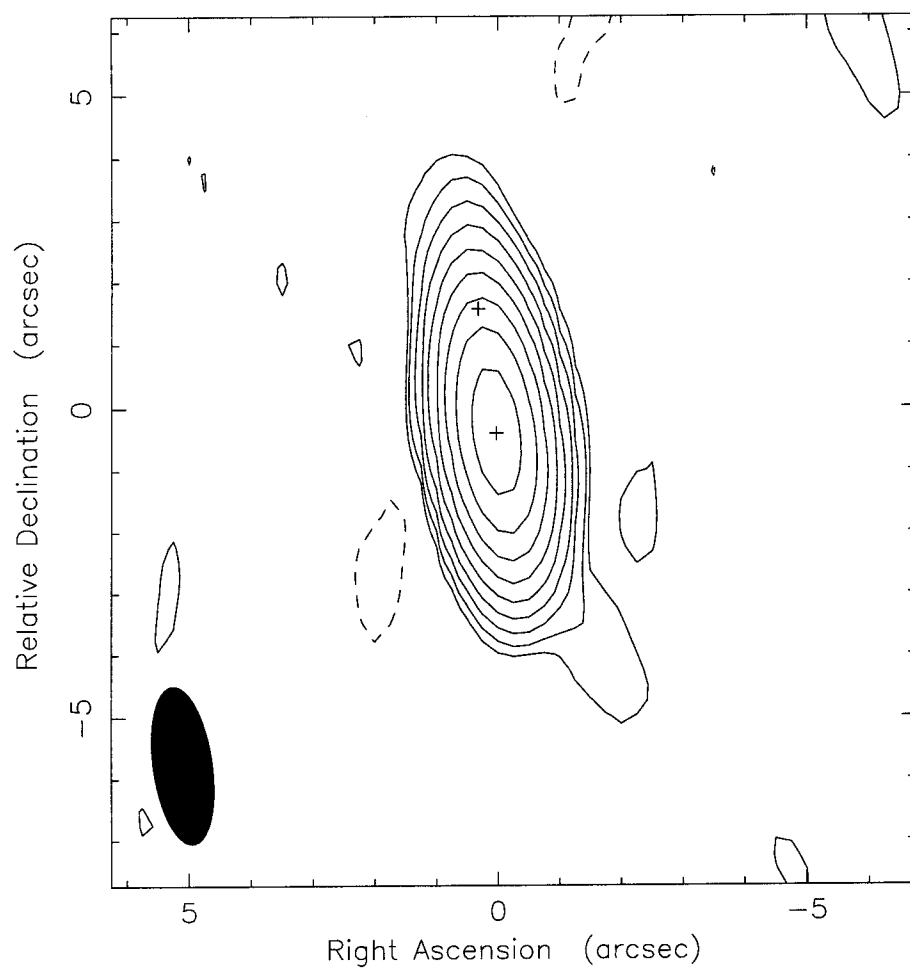


Fig. 1.—

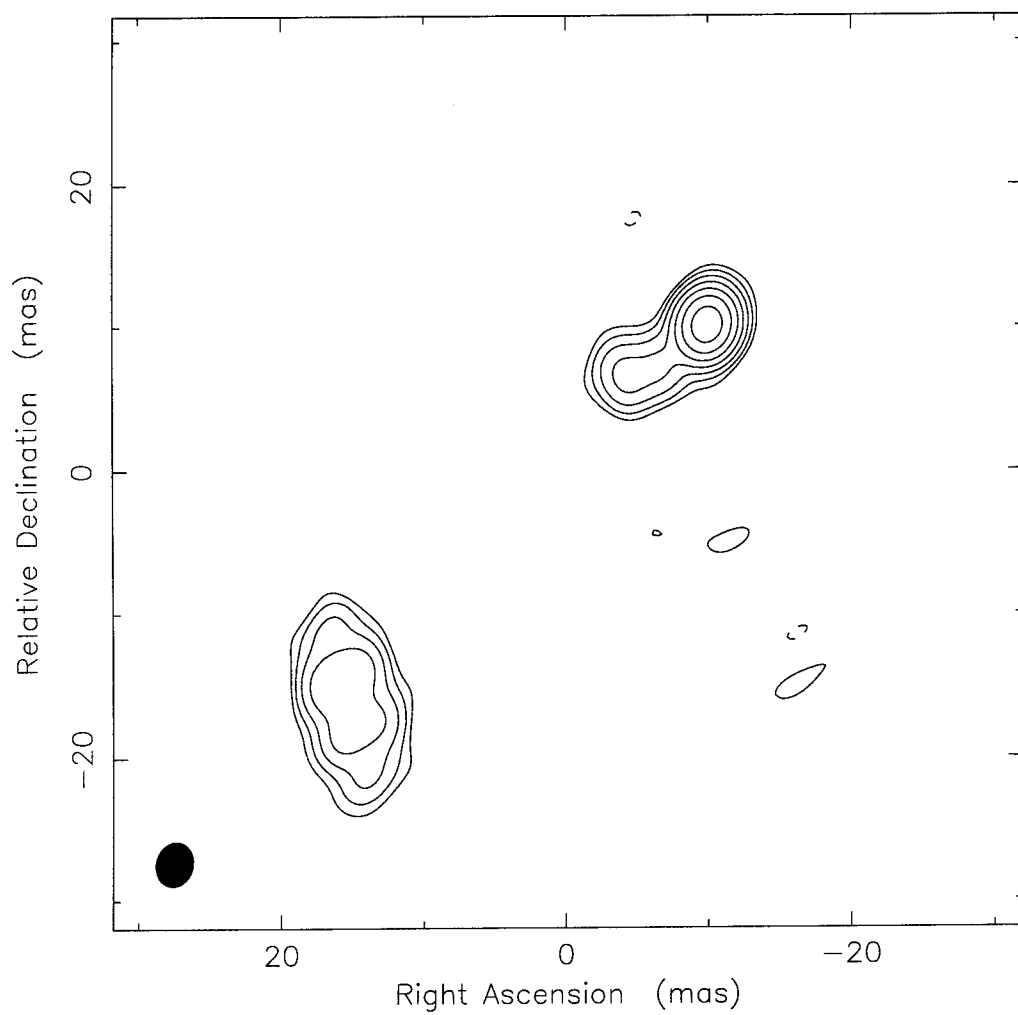


Fig. 2.—

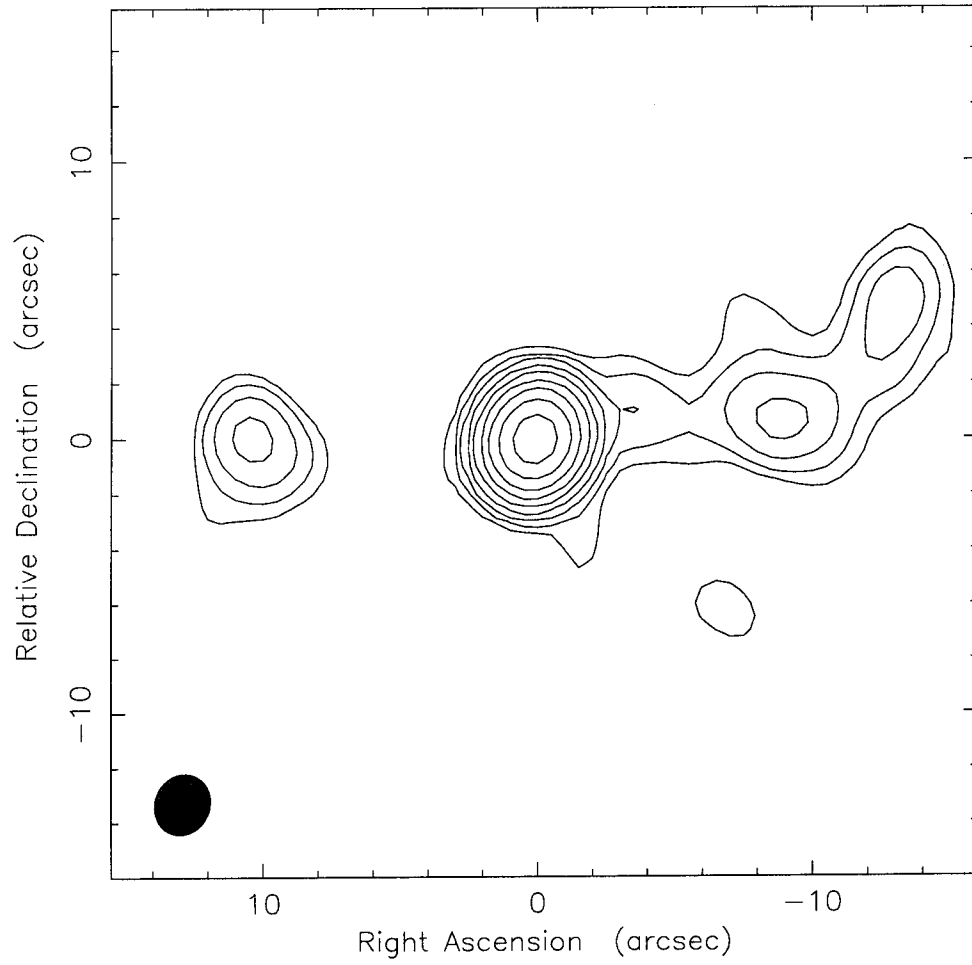


Fig. 3.—

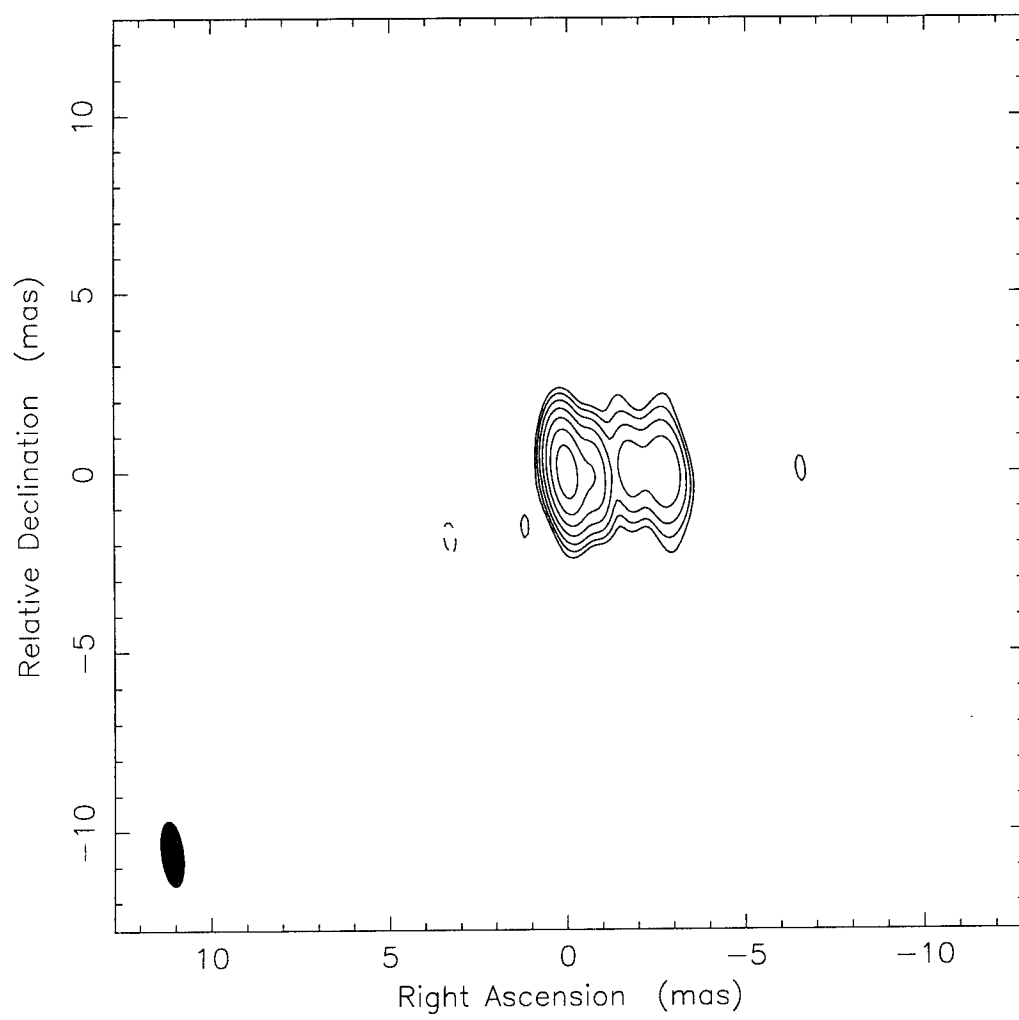


Fig. 4.—

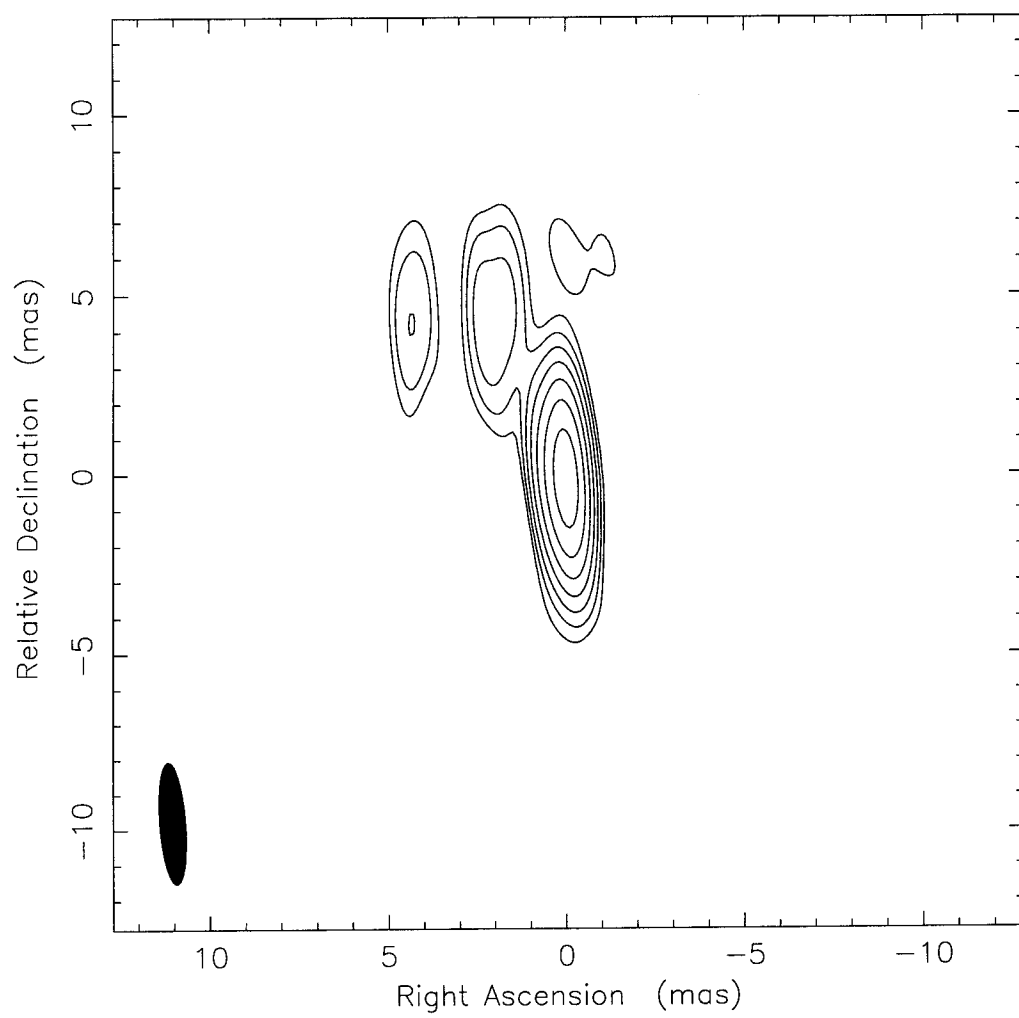


Fig. 5.—